JOURNAL OF MATERIALS SCIENCE 29 (1994) 1449–1454

Crystallization mechanism of amorphous $Ni_{65}Cr_{16}P_{19}$ metallic alloys

KOUJI MAEDA, TETSUO IKARI, YOSHITO AKASHI*, KOJI FUTAGAMI
*Departments of Electronics and *Applied Physics, Miyazaki University 1-1 Gakuenkibanadai, Miyazaki 889-21, Japan*

Two large exothermic reaction peaks at 658 and 690 K are observed in the differential scanning calorimetric (DSC) curve for the amorphous metallic alloy, $Ni_{65}Cr_{16}P_{19}$. Extensive DSC and X-ray diffractometer measurements were carried out for pre-annealed samples, and it is concluded that the two peaks are due to crystallization of Ni and stable Ni_3P phases, respectively. The expanded lattice constants of these phases can be explained by assuming that a small amount of Cr atoms were dissolved in these crystalline phases. As for the metastable Ni_3P phase, confirmation of its presence by X-ray measurement could not be obtained. These results may be interpreted by considering that the metastable phase appears only in the thin film region of the sample.

1. Introduction

Amorphous metallic alloy is well known as a new material which has high magnetic permeability and excellent resistance to corrosion. Since these characteristics of amorphous alloys deteriorate drastically during crystallization, investigation of the crystallization kinetics has been extensively studied. Further attention has been paid to the appearance of metastable crystalline phases during crystallization of the amorphous materials. This is because these metastable phases could not be obtained by usual crystal growth techniques. A comparison of the crystallization process for the metastable phase with that for the stable phase may give an insight into the detailed kinetics of nucleation and atom diffusion mechanisms in the amorphous materials.

A two phase mixture of Ni and Ni_3P was known to be present during the crystallization process of a metallic amorphous Ni–P alloy system. The stable Ni_3P phase has a body centred tetragonal (b.c.t.) crystal structure, with lattice constants of $a = 0.8954$ nm and $c = 0.4386$ nm [1]. The metastable crystalline phases were observed by transmission electron microscope (TEM) measurements during crystallization of amorphous Ni–P alloy, or Ni–P based ternary alloys. However, discussion of their structures and compositions are still controversial. For $Ni_{68.5}Cr_{14.5}P_{17}$ metallic alloy, Conde *et al.* [2] reported preliminary results of differential scanning calorimetric (DSC) measurements. They showed that the Ni–Cr and $(Ni,Cr)_3P$ crystalline phases grow from the amorphous phase by continuous heating; and, no indication for the appearance of the metastable phase, which is commonly observed in these metal–metalloid systems, was given. In this paper, detailed experimental results from DSC and X-ray diffraction measurements for amorphous $Ni_{65}Cr_{16}P_{19}$ metallic alloy are reported, especially on samples which were subjected to pre-annealing at temperatures below and above the crystallization temperature prior to measurement. The presence of metastable and stable crystalline Ni(Cr) phases will be confirmed, and the role of Cr atoms in the crystallization mechanism will be discussed. It is also suggested that the metastable Ni_3P phase with hexagonal symmetry, observed in the TEM measurements, does not appear in the bulk samples.

2. Experimental procedure

Quenched amorphous $Ni_{65}Cr_{16}P_{19}$ (a-NiCrP) alloy ribbon of 40 μm thickness were obtained from Allied Chemical Co. Ltd. The composition of the alloys was checked by energy dispersive X-ray spectrometer (EDX) measurements. Cobalt atoms, of 0.8 at %, were included in the samples as an impurity. The ribbons were pre-annealed in vacuum by continuous heating at a rate, ϕ, of 10 K min^{-1} to the desired temperature; the ribbons were then quenched in water. Measurement of the crystallization temperatures for as-received and pre-annealed samples were performed by DSC. The samples, 1.5–2.0 mg, sealed in Al sample pans, were placed in the calorimeter, and an N_2 gas flow was used for the ambient atmosphere. The absolute temperature of the calorimeter was calibrated by checking the melting points of lead and tin at 600.6 and 505.1 K, respectively.

Selected area electron diffraction (SAD) measurements were carried out using 200 kV TEM. Samples for the TEM study were prepared by jet-polishing in a Tenupol apparatus; with concentrated acetic acid plus perchloric acid, in the volume ratio 7:3, as the electrolyte. Pre-annealing treatments were always performed after jet-polishing, since selective etching was recognized when the pre-annealed samples were subsequently polished.

0022–2461

X-ray diffractometer measurements, to estimate the lattice constant precisely, were carried out for the as-received and pre-annealed samples by CuK_α radiation with a Ni filter. Powder samples were obtained by grinding the heat treated alloy ribbons to a particle size of $\sim 90\,\mu m$. Calibration of the lattice constants was carried out using Si powder as a reference material.

3. Results

Compositional analysis by EDX shows that the ratio of Ni to Cr is always four for the samples pre-annealed below 770 K. This indicates that these atoms were uniformly distributed, as is the case for the amorphous phase. For the annealed samples, above 770 K, a region with a high concentration of Cr appeared in the matrix. However, no distinctive evidence of the segregation of Cr atoms could be observed from the SAD patterns.

Only a broad halo was observed in the SAD pattern for the as-received samples. This indicates that the as-received samples were in an amorphous state. A SAD pattern with a six-fold symmetry was observed for the samples pre-annealed at 643 K. This shows that a metastable Ni_3P phase, with hexagonal symmetry, appears at this annealing temperature. The estimated lattice constant, $a = 0.463$ nm, is slightly larger than that of the metastable Ni_3P phase observed in the Ni–P system [3]. This metastable phase disappeared for samples annealed above 720 K. Furthermore, above the pre-annealing temperature of 660 K, thin rings corresponding to fine Ni particles overlay the broad halo of the amorphous phase in the SAD pattern. These rings became clearer when the annealing temperature increased. For samples annealed around 690 K, SAD patterns with four-fold symmetry were observed. These diffraction spots are due to the stable b.c.t. phase of Ni_3P crystals [3].

Fig. 1 shows the DSC curve of the as-received a-$Ni_{65}Cr_{16}P_{19}$ sample, with a heating rate, ϕ, of $10\,K\,min^{-1}$. Two large exothermic reactions were observed. The lower temperature peak (hereafter referred to as the first peak) starts at 651 K, and has a maximum at 658 K. The higher temperature second peak starts at 685 K, with a maximum at 690 K. The rise up temperature for the second peak is not clear because of strong tailing of the first peak. Both peaks shift to the lower temperature side when the heating rate decreases. The enthalpies of the transformations for the first and the second peaks estimated from integrated intensities of the exothermic peaks, are 23 and 47 $kJ\,mol^{-1}$, respectively.

In addition to these two sharp peaks, fine structures are observed in the tail regions. To clarify these structures, expanded DSC curves, multiplied by a factor of 20, are also shown in the Fig. 1. Below the first peak, a broad and weak exothermic reaction band is observed above 450 K. This exothermic band is considered to be due to a change in the microstructure of the amorphous phases. A smaller, but distinctive, endothermic reaction at 626 K, indicated by the arrow in the Fig. 1, is also shown in the expanded DSC curve.

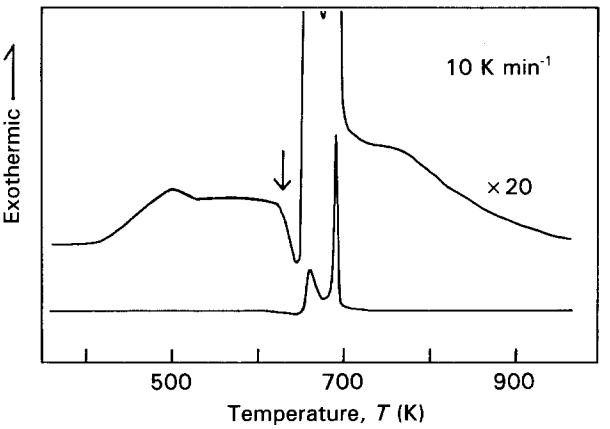

Figure 1 DSC curve for a-NiCrP alloy at a heating rate of $10\,K\,min^{-1}$. The expanded curve is shown.

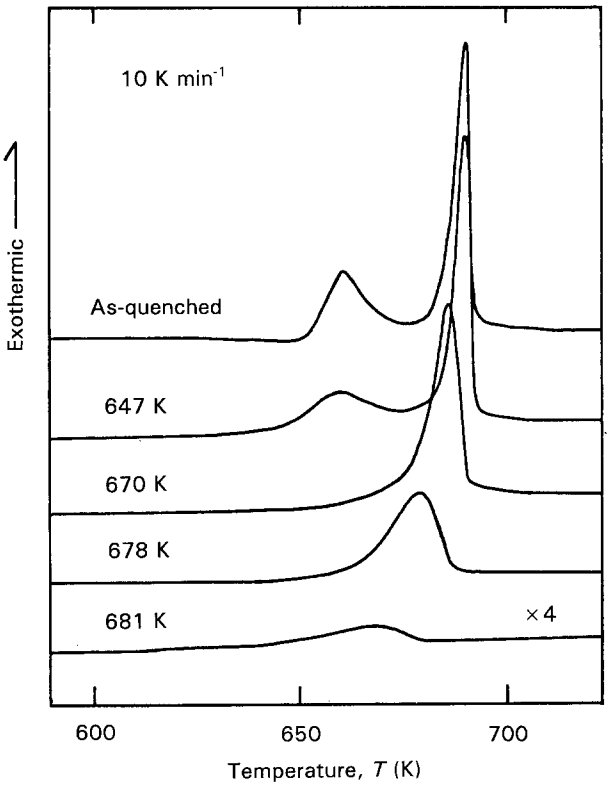

Figure 2 Pre-annealing temperature dependence of the DSC curve for a-NiCrP at a heating rate of $10\,K\,min^{-1}$.

This endothermic reaction is truncated by the subsequent exotherm (the first peak), with quite large intensity. As in the case for many metallic glasses [2], this may be assigned to transition from the glass state to the supercooled liquid phase. Details are discussed in the next section.

Fig. 2 illustrates the DSC curves for the pre-annealed sample; heated at $\phi = 10\,K\,min^{-1}$ to the desired temperature, which characterizes the degree of crystallization. The pre-annealed temperatures are, thus, taken as parameters. At a pre-annealing temperature of 647 K, which is lower than the first peak temperature in the DSC curve of the as-received sample, the height of the first peak becomes smaller and the temperature peak shifts to the lower temperature side. However, the shape and the peak temperature of the second peak remain unchanged. This indicates that pre-annealing below the first peak temperature does not interfere with the second peak.

When the samples were pre-annealed from 670 to 681 K, i.e. the region between the first and the second peak, the first peak disappeared completely. The heights and the peak temperatures of the second peak become smaller with increased pre-annealing temperature. For the samples pre-annealed above 688 K, no peak due to crystallization occurs.

It is well known that the activation energies of crystallization are determined by Kissinger's plot of $\ln[\phi/T^2]$ versus $1/T$; where ϕ is the heating rate, and T is the reaction starting temperature observed in the DSC curves [4]. The starting and the peak temperatures of the first and the second peak were measured by changing the heating rate, ϕ, from 0.167 to 20 K min^{-1} for the as-received samples. The observed Kissinger's plots are shown in Fig. 3. All the data points for the first peak fall on a straight line, with an estimated activation energy (ΔE) of 360 kJ mol^{-1}. The activation energy for the second peak is also determined to be 333 kJ mol^{-1}. Similar analyses of the activation energies were also carried out for samples pre-annealed at different temperatures. The activation energies, as a function of pre-annealing temperatures, are shown in Fig. 4. Both activation energies for the first and the second peak decrease as the pre-annealing temperature increases. No peak corresponding to the first peak appears for the samples pre-annealed above 670 K as discussed above.

Fig. 5 shows the X-ray diffraction patterns for the samples pre-annealed at different temperatures. No distinctive diffraction line is observed for the samples heated up to 597 K. Their diffraction patterns are well characterized by a broad halo, which implies that the samples are in an amorphous phase. For the sample pre-annealed at 655 K, which characterizes the starting temperature of the first exothermic peak in the DSC curve, the maximum, of the halo shift to the low diffraction angle side and a tiny peak appears at $2\theta = 44.5°$. This diffraction angle coincides with the (111) diffraction of a face centred cubic (f.c.c.) Ni crystal. This shows that small Ni precipitates exist around the first exothermic peak. Many diffraction lines appear for the samples pre-annealed at 690 and 793 K. The former and the latter temperatures correspond exactly at, and far above, the second peak, respectively. The halos which characterized the amorphous phase still remain. The observed diffraction lines are well assigned to the mixture of the f.c.c. Ni and stable b.c.t. Ni_3P crystalline phases. Typical Miller indices for the diffraction lines are indicated in Fig. 5. Considerable amounts of Ni precipitates and the stable Ni_3P phase crystallizes, above 690 K. The lowest pattern in Fig. 5 is for a completely crystallized sample, which is obtained by annealing at 876 K for 24 h. The diffraction lines for the Ni crystal become large compared with that of the Ni_3P phase. No evidence for the presence of a metastable Ni_3P phase is observed by present X-ray diffraction measurements.

The observed lattice constants of f.c.c. Ni and b.c.t. Ni_3P crystals, estimated from the X-ray diffraction angle as a function of pre-annealing temperature, are

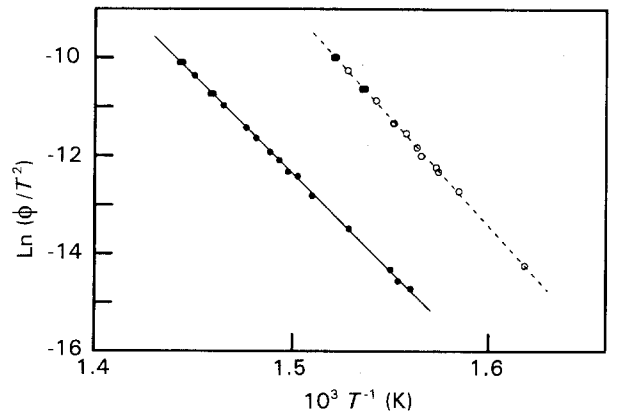

Figure 3 Kissinger's plot of ln (ϕ/T^2) versus $1/T$ for a-NiCrP. Activation energies (ΔE) for the first (○) and second (●) peak are estimated as 360 and 333 kJ mol^{-1}, respectively.

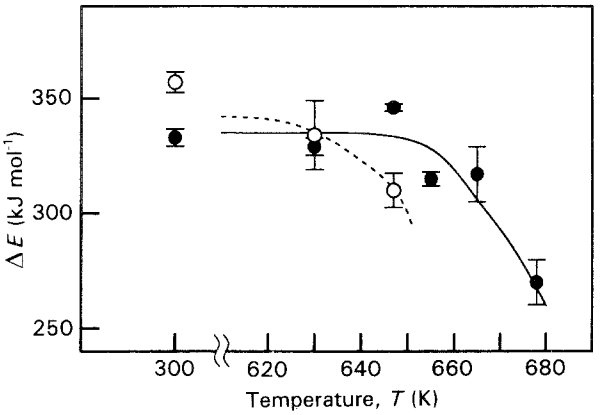

Figure 4 Pre-annealing temperature dependence of the estimated activation energies by Kissinger's plot. (○) first peak, (●) second peak.

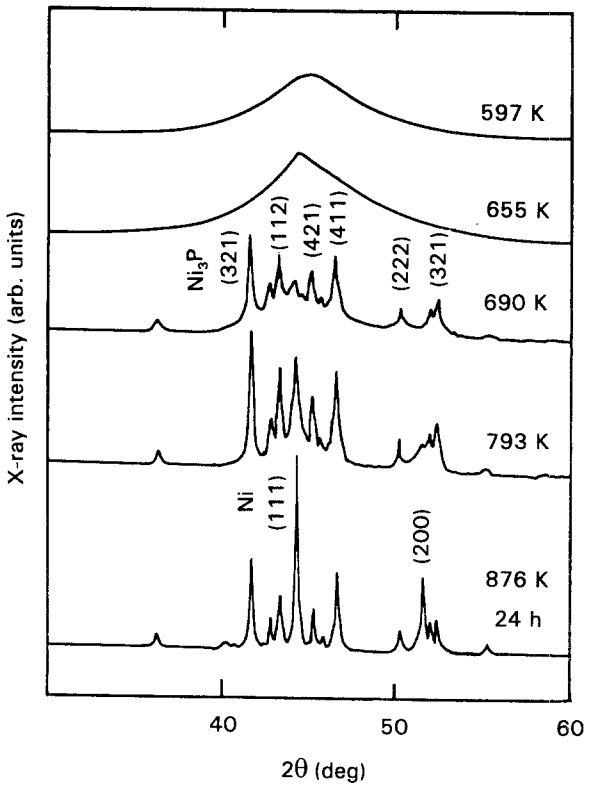

Figure 5 X-ray diffraction patterns of samples continuously heated up to different temperatures. Annealing at 876 K for 24 h completely crystallizes the sample.

shown in Fig. 6. The lattice constant of Ni decreases with annealing temperature, from 669 to 693 K, and becomes constant at 0.3542 nm above 790 K. For the stable Ni_3P crystal, lattice constants a and c increase gradually with annealing temperature. They are 0.8958 and 0.4423 nm, respectively, for the sample pre-annealed at 680 K.

The X-ray diffraction patterns in Fig. 5 are decomposed numerically into three components, i.e. f.c.c. Ni, stable b.c.t. Ni_3P crystals and amorphous phases. Supposing that the integrated X-ray diffraction intensity is proportional to the total amount of each phase involved in the sample, then the annealing temperature dependence of the fractional compositions of these phases can be estimated. They are shown in Fig. 7 as a function of pre-annealing temperature. The (111) diffraction line for Ni, and (321) and (411) for Ni_3P, were typically used for the calculation. The intensity of the amorphous phase was determined from the area of the halo by subtracting the background signal. Above 680 K, the fraction of the stable Ni_3P phase abruptly increases and shows a plateau above 680 K. This indicates that almost all of the stable Ni_3P phase grows within a narrow temperature range of the second peak. However, the Ni phase gradually increases above 680 K, and continuously increases up to the maximum temperature of the present experiment. The amorphous phase decreases with increasing pre-annealing temperature, in the range between the first (658 K) and the second peak (690 K). Note that small amounts of the amorphous phase still exist at temperatures as high as, say, 800 K.

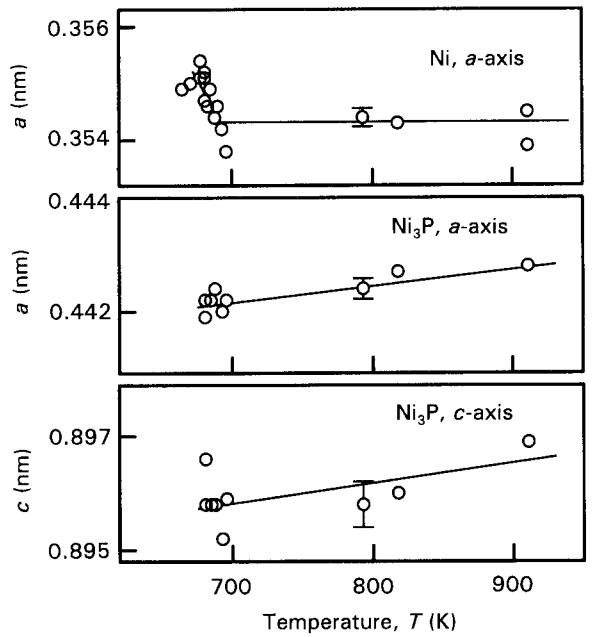

Figure 6 Annealing temperature dependence of the lattice constant for Ni and stable Ni_3P crystals.

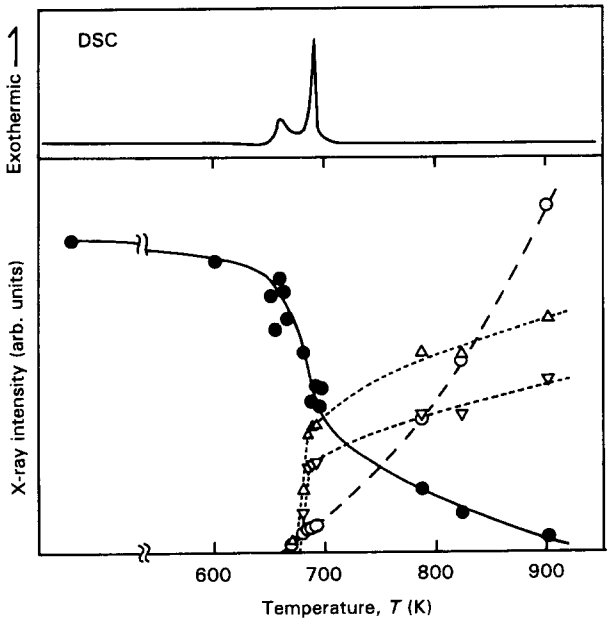

Figure 7 Annealing temperature dependence of relative X-ray diffraction peak intensity. This is considered to be proportional to the volume fraction of crystals. Note that the amorphous phase still remains even above 800 K. (●) amorphous, (○) Ni (111), (△) Ni_3P (321), (▽) Ni_3P (411).

4. Discussion

4.1. Crystallization mechanism

Below the first peak, a broad and weak exothermic reaction band is observed above 450 K, as shown in Fig. 1. This exothermic band is considered to be due to changes in the microstructure of the amorphous phases. A certain kind of atomic rearrangement occurs in this temperature range. Such structural changes at an atomic scale can exist even when the matrix still remains in an amorphous state. A similar weak exothermic band, just below the narrow exothermic peak in the DSC curve, was observed in Fe–Ni based alloys by Chang and Sastri [5]. They considered that the first DSC precipitation peak of small Ni particles, before the onset of crystallization, may cause the structural change and the weak exothermic reaction. However, no evidence for precipitation of Ni crystals was obtained by the X-ray measurements presented here. This could be explained by supposing that the particle sizes of the Ni precipitates were too small to be detected by the X-ray equipment. Although a detailed mechanism is not clear at present, it would be reasonable to consider that some sort of atomic rearrangement occurred in this temperature region.

A small, but distinctive, endothermic reaction at 625 K was attributed to glass transition from the amorphous to the supercooled liquid phase. Conde *et al.* [2] observed a similar glass transition in their DSC curve for $Ni_{68.5}Cr_{14.5}P_{17}$ amorphous metallic alloy. Their reported glass transition temperature is slightly larger than that given here. Since the composition of Conde *et al.*'s constituent atoms is quite similar to that of the samples in this experiment, the difference observed between the glass transition temperatures needs to be explained. It is considered that the difference is due to the different heating rates employed to obtain the DSC curves. The larger heating rates inducing the larger glass transition temperatures.

Similarly, two large exothermic peaks in the DSC curve were obtained by Thorpe *et al.* [6] for $Fe_{40}Ni_{40}P_{14}B_6$ metallic amorphous alloys. They attributed these two peaks to the crystallization of two metastable (MS) phases (MS-I and MS-II for low and

high temperature peaks) from the amorphous matrices. Inspite of an extensive investigation into the crystal structure of these metastable phases, no definitive structure nor composition were elucidated. It is well known that the two MS phases transform to the stable crystalline phase by successive heating [7]. These characteristics are generally accepted for crystallization processes of the ternary metal–metalloid–amorphous alloys.

The first exothermic peak starts steeply at 651 K, and has a maximum at 658 K. The glass transition is not accomplished in this temperature region. The X-ray diffraction pattern for the 655 K annealed sample shows a tiny peak near the top of the amorphous halo. Since the diffraction angle of 44.8° 2θ is close to the (111) diffraction line of the Ni crystal, it is considered that crystallization of Ni atoms induces the first peak. A metastable Ni_3P phase (MS Ni_3P), with hexagonal symmetry, was observed in this temperature region by TEM analysis, as stated above. However, confirmation of the presence of the metastable Ni_3P phase by X-ray measurement could not be observed. These results may be interpreted by assuming that the MS Ni_3P phase only appears in the thin film region of the sample. The samples for TEM measurement are usually perforated and have wedge-shaped regions around the hole to transmit the electron beam effectively. Past reports on the appearance of metastable phases were all investigated by TEM measurement. The surfaces of the thin film may prohibit crystal growth of the stable Ni_3P phase, and advance the crystallization of the metastable phases. In an early investigation of the Ni–P amorphous system [3], the activation energies, ΔE, for crystal growth were determined by Kissinger's plot. The observed ΔE for the metastable Ni_3P phase is larger for thin film samples (3.1 eV) than for the bulk samples (2.3 eV). These experimental results also support considerations made here for the present Ni–Cr–P system. The metastable phase could not appear in the bulk samples.

The second peak starts to increase near 685 K, and has a maximum at 690 K. Above these temperatures, the stable Ni_3P phase grows rapidly followed by a gradual increase. The amount of the amorphous phase decreases in the same temperature region, as shown in Fig. 7. The TEM results also indicate that the Ni_3P stable phase grew rapidly in these temperature regions. The stable Ni_3P phase grows within a narrow temperature range of the second peak.

It should be noted that the amorphous phase remains up to a surprisingly high temperature of 800 K. Therefore, when the as-received sample was heated up to 700 K and then quenched to room temperature, an appreciable fraction of the amorphous phase should remain in the sample (hereafter referred to as the residual amorphous phase). DSC measurements were carried out up to 900 K for this pre-annealed sample consisting of residual amorphous phases. No peak corresponding to the two sharp exothermic peaks, as shown in Fig. 1, could be observed. These facts indicate that the residual amorphous phase is more stable than the amorphous phase in the as-received samples, with respect to composition and structure. No crystallization occurs even when the DSC curve traces up to 900 K. If it is considered that when the residual amorphous phase exists within a narrow region among the crystalline phases, such as Ni and stable Ni_3P phases in this case, the activation energy of crystallization becomes large. The diffusion of the constituent atoms may be prohibited in these restricted regions. Therefore, the crystallization exotherms in the DSC curve could not be obtained.

4.2. Change of lattice constants

The lattice constant of Ni crystals having a f.c.c. structure is reported to be 0.3524 nm [8] and this value is considerably smaller than that of the present experiments (0.3542 nm), as shown in Fig. 6. Since Ni–Cr alloy forms a solid solution in the compositional range of interest, the lattice constant slightly increases to 0.3528 nm when the 22 at % of Cr atoms is dissolved in the Ni crystal [9]. This fraction of Cr to Ni, 22 at %, is almost the same as the ratio of the present alloy system of $Ni_{65}Cr_{16}P_{19}$. This shows that increase of the lattice constant would be ~ 0.0004 nm. Therefore, the larger lattice constant of the Ni crystalline phase, below 696 K in Fig. 6, is explained by substitution of Cr atoms into the Ni atom sites. The invariance of the lattice constant above 696 K indicates that the Cr atoms were saturated in the Ni phase. It is unlikely that Cr atoms further substitute the Ni atom sites by pre-annealing in this temperature range.

The Ni lattice constant decreases with the pre-annealing temperature below 696 K, as shown in Fig. 6. This may be explained by assuming that the density of the Ni crystal phase becomes large with the increase of pre-annealing temperature. The most dense form of Ni crystals appear above 696 K. Therefore, it is considered that a metastable Ni crystalline phase, with a larger lattice constant, appears at the temperature of the first exothermic peak (658 K) and becomes more stable up to 696 K. The strong first peak at 658 K, in the DSC curve in Fig. 1, is due to the formation of a metastable Ni crystalline phase. Since the Cr atoms easily dissolve in the Ni phase, this metastable Ni phase should contain a certain fraction of the Cr atoms. In the case of $Ni_{81}P_{19}$ amorphous alloy, which has a nearly equal metal–metalloid ratio as in the present experiment, only one dominant peak was observed at 642 K in the DSC curve [3]. One of the differences of the crystallization features between Ni–P and Ni–Cr–P alloys is considered to be due to the fact that part of the Ni atomic site is substituted by the Cr atom. However, why two peaks appear in the N–Cr–P systems is open to question. The diffusion of P and Ni atoms may be influenced by the presence of Cr atoms.

The lattice constant of the stable Ni_3P phase, which has a b.c.t. structure, is reported to be $a = 0.8925$ nm and $c = 0.4388$ nm [8]. The results in Fig. 6 show that the lattice constants are larger than their reported value by 0.2% and 1% for the a and c axes, respectively. Furthermore, these lattice constants increase considerably with the increase in pre-annealing temperature. If it is assumed that the Cr atoms dissolve in

the Ni_3P phase, and substitute for the Ni atoms, the lattice expansion may be estimated to be as large as ~ 0.0004 nm for lattice constant a, as discussed above. This is a reasonable variation of the lattice constant for the experimental results shown in Fig. 6. However, the difference between the experimental results and the assumed value is not reasonable for c. The lattice expansion may be due to substitution of the Cr atoms for Ni atom sites in the crystalline Ni_3P phase. A detailed mechanism for this substitution is not clear at present.

4.3. Activation energies

The apparent activation energies of crystallization (ΔE) in a-$Ni_{68.5}Cr_{14.5}P_{17}$ alloys were investigated by Conde *et al.* [2]. They determined ΔE of 404 and 368 kJ mol^{-1} for the first and second exothermic crystallization peaks, respectively. The results of 360 and 333 kJ mol^{-1} reported here are about 10% smaller. As stated above, the amorphous Ni–P binary alloy system has one dominant exothermic peak. The obtained ΔE for the $Ni_{81}P_{19}$ and $Ni_{80}P_{20}$ systems are 262 kJ mol^{-1} [3] and 216 kJ mol^{-1} [4], respectively. For the commercially available amorphous alloy of 2826A ($Fe_{32}Ni_{36}Cr_{14}P_{12}B_6$), two exothermic peaks due to crystallization were reported by Thorpe *et al.* [6]. They observed ΔE of 186 and 543 kJ mol^{-1} for the first lower temperature and the second higher temperature peak, respectively. The bonding state of metal and metalloid in amorphous phases may drastically affect the activation energies of crystallization. The activation energies become larger when the number of constituent atoms increases.

The activation energy, ΔE, for the first peak decreases with the increase of pre-annealing temperature above 647 K, as shown in Fig. 4. For the as-received samples, the activation energy of crystallization consists of two contributions. They are the activation energy for crystal nucleation and that for crystal growth, e.g. diffusion and stacking of the atoms. Above the glass transition temperature of 625 K, the viscosity of the super-cooled amorphous liquid becomes smaller; and accordingly, diffusion of the constituent atoms becomes easier. Therefore, a number of the Ni nuclei appear and the structure becomes more relaxed for the samples pre-annealed at 647 K. This leads to a decrease in the activation energy for the first peak. The contribution from the activation energy of nucleation diminishes when the pre-annealed samples undergo subsequent DSC measurement.

The activation energy of the second peak of stable Ni_3P crystallization also decreases above the pre-annealed temperature of 670 K. The reason for this decrease is similarly considered to be due to an increase in the number of nuclei of stable Ni_3P crystals present. At the pre-annealing temperature of 670 K, nuclei of Ni_3P crystals appear in the sample. Therefore, the activation energy decreases in the same manner, as is the case for the first peak.

5. Conclusions

Two large exothermic reaction peaks at 658 and 690 K (referred to as the first and second peaks) and accompanying fine structures in the DSC curve for the amorphous metallic alloy, $Ni_{65}Cr_{16}P_{19}$ were observed. Extensive DSC and X-ray diffractometer measurements were carried out for the pre-annealed samples in order to discuss the origin of these peaks. Pre-annealing temperatures were chosen to characterize the crystallization stages that appeared in the DSC curve of the as-received samples. Since the diffraction line of the f.c.c. Ni crystal appears in the X-ray chart for the sample pre-annealed at 658 K, it was considered that crystallization of the Ni phase induced the first peak. The larger lattice constant, a, of the Ni phase, than that of the reported value, can be explained by assuming that a small amount of Cr atoms were dissolved in the f.c.c. crystalline phase. This Ni phase becomes more stable with increasing temperature, and induces the decrease of a from the first peak temperature to about 700 K.

The second peak is attributed to crystallization of the stable Ni_3P phase with a b.c.t. crystal structure. The lattice constants a and c both increase with temperature. These increases are partly explained by assuming that the Cr atoms dissolve in the Ni site of the Ni_3P crystal phase and expand the lattice. As for the metastable Ni_3P phase previously observed in the TEM measurements, confirmation of the presence of such a phase by X-ray measurement could not be obtained. These results may be interpreted by considering that the metastable Ni_3P phase only appears in the thin film region of the sample. The surfaces of the thin film may prohibit crystal growth of the stable Ni_3P phase and advance the crystallization of the metastable phases.

The apparent activation energies, ΔE, for the first and the second DSC peaks are estimated using Kissinger's plot for the as-received and pre-annealed samples. They decrease with an increase in the pre-annealing temperature around the exothermic peaks in the DSC curve. Since ΔE consists of activation energy for nucleation and that for crystal growth, it decreases when nucleation proceeds during the pre-annealing treatment.

References

1. E. VAFAEI-MAKHSOS, *J. Appl. Phys.* **51** (1980) 6366.
2. C. F. CONDE, H. MIRANDA, A. CONDE and R. MARQUEZ, *J. Mater. Sci.* **24** (1989) 139.
3. T. IKARI, M. IZAKI, T. FUKUMORI and K. FUTAGAMI, *ibid.* **26** (1991) 583.
4. K. LU and J. T. WANG, *ibid.* **23** (1988) 3001.
5. H. CHANG and S. SASTRI, *Metallurgical Trans.* **8A** (1977) 1063.
6. S. J. THORPE, B. RAMASWANI and K. T. AUST, *Acta Metall.* **36** (1988) 795.
7. A. INOUE, T. MASUMOTO and M. KIKUCHI, *J. Japan Inst. Metals* **42** (1978) 294.
8. M. L. SUI, K. KU and Y. Z. HE, *Phil. Mag.* **B63** (1991) 993.
9. L. KARMAZIN, *Czech. J. Phys.* **B29** (1979) 1181.

Received 3 August 1992
and accepted 31 August 1993